Eur. Phys. J. A **28**, 295–299 (2006)
DOI 10.1140/epja/i2006-10058-0

THE EUROPEAN PHYSICAL JOURNAL A

Scattering of ^{11}Be halo nucleus from ^{209}Bi at the Coulomb barrier

M. Mazzocco[1], C. Signorini[1,a], M. Romoli[2], A. De Francesco[2], M. Di Pietro[2], E. Vardaci[2], K. Yoshida[3], A. Yoshida[3], R. Bonetti[4], A. De Rosa[2], T. Glodariu[1,5], A. Guglielmetti[4], G. Inglima[2], M. La Commara[2], B. Martin[2], D. Pierroutsakou[2], M. Sandoli[2], F. Soramel[6], L. Stroe[5,7], R. Kanungo[3,8], N. Khai[3], T. Motobayashi[3], T. Nomura[9], T. Ishikawa[9], H. Ishiyama[9], S. Jeong[9], H. Miyatake[9], M.H. Tanaka[9], I. Sugai[9], and Y. Watanabe[9]

[1] Dipartimento di Fisica and INFN, via Marzolo 8, I-35131, Padova, Italy
[2] Dipartimento di Scienze Fisiche and INFN, Complesso Universitario di Monte S. Angelo, via Cinthia, I-80125, Napoli, Italy
[3] The Institute of Physical and Chemical Research (RIKEN), Wako-shi, Saitama, 351-0198, Japan
[4] Istituto di Fisica Generale ed Applicata and INFN, via Celoria 16, I-20133, Milano, Italy
[5] National Institute for Physics and Nuclear Engineering - "Horia Hulubei", 407 Atomistilor st., 077125, Magurele, Romania
[6] Dipartimento di Fisica and INFN, via delle Scienze 208, I-33100, Udine, Italy
[7] INFN - Laboratori Nazionali di Legnaro, viale dell'Università 2, I-35020, Legnaro (Padova), Italy
[8] TRIUMF, 4004 Wesbrook Mall, Vancouver, Canada
[9] Institute of Particle and Nuclear Studies (KEK), 1-1 Oho, Tsukuba-shi, Ibaraki, 305-0801, Japan

Received: 27 March 2006 / Revised: 10 May 2006 /
Published online: 14 July 2006 – © Società Italiana di Fisica / Springer-Verlag 2006
Communicated by Th. Walcher

Abstract. The scattering of the radioactive, weakly bound, halo nucleus ^{11}Be from ^{209}Bi has been studied at 40 MeV beam energy. The measurement performed with a low-intensity and a large-emittance secondary beam could be made using an extremely compact, large solid angle ($\sim 2\pi$ sr) detecting set-up, based on 8 highly segmented Si telescopes. The ^{11,9}Be scattering angular distributions, as well as their relative reaction cross-sections, resulted to be rather similar. This may suggest that at Coulomb barrier energies the halo structure and the very small binding energy of the ^{11}Be projectile have no big influence on the reaction dynamics.

PACS. 25.60.Bx Elastic scattering – 25.60.Dz Interaction and reaction cross-sections – 27.20.+n $6 \leq A \leq 19$

Nuclear reactions induced by light loosely bound radioactive ion beams are expected to show new effects in the reaction dynamics around the Coulomb barrier. In this framework the measurement of the elastic scattering differential cross-sections plays an important role since it provides basic information on the interaction potential of the colliding nuclei and consequently on the reaction cross-section σ_{re}. These data are relevant since, in this energy range, few reaction processes, namely fusion and those processes originating from the very small binding energy of the projectile like the breakup, are expected to contribute to this cross-section. Extended theoretical work is proceeding on these topics (see, *i.e.*, refs. [1,2]).

This work presents the results of the ^{11}Be scattering from a ^{209}Bi target around the Coulomb barrier. ^{11}Be has some characteristic features: $T_{1/2} = 13.8$ s, $S_n = 504$ keV, only one bound excited state at 320 keV and a well-established halo structure with a r.m.s. radius 10% larger than systematics [3]. In this region similar experiments have been performed with the following weakly bound projectiles: ^{6}He, $T_{1/2} = 0.80$ s, $S_{2n} = 972$ keV, neutron skin-like structure; ^{17}F, $T_{1/2} = 64.6$ s, $S_p = 601$ keV; ^{9}Be, stable, $S_{2\alpha+n} = 1574$ keV. The system ^{6}He + ^{209}Bi [4,5] has a big σ_{re}, much larger than the fusion one, originating from a very strong α channel [5] attributed to the ^{6}He (inclusive) breakup process, while for ^{17}F + ^{208}Pb the σ_{re} [6] is very similar to the total fusion one [7] and the ^{16}O production (inclusive breakup) has a cross-section [8] much smaller than the total fusion. Also for the system ^{9}Be + ^{209}Bi there is a strong (inclusive breakup) α channel [9], whose strength is comparable to the fusion one and their sum exhausts the σ_{re} [10].

In this scenario the measurement of the differential cross-section for the scattering of ^{11}Be from ^{209}Bi is a very good link between the two radioactive beams, since ^{11}Be has a binding energy as small as ^{17}F and a halo structure similar to ^{6}He. Moreover, for the system ^{11}Be + ^{209}Bi the fusion process has already been measured around the bar-

[a] e-mail: signorini@pd.infn.it

rier and the cross-sections resulted to be very similar to the ^{9,10}Be + ^{209}Bi ones [11], contrary to simple expectations. This feature suggests moderate breakup effects.

The experiment was performed at the RIPS fragment separator [12] in RIKEN. The ^{11}Be secondary beam was produced at 66.1 A·MeV via fragmentation of a $^{13}C^{6+}$ primary beam, 101.2 A·MeV energy, with $\sim 3\,\mu$A current on a 12 mm thick Be plate. The secondary beam was subsequently reduced in energy by two Al degraders (6 mm and 5 mm thick, respectively) and eventually refocused with a quadrupole triplet on the secondary reaction chamber. Two Parallel Plate Avalanche Counters (PPACs) [13] were located along the beam line at a distance of 30.4 cm from each other. The target was located 68.2 cm downstream the closest PPAC. Both PPACs were x-y position sensitive with a resolution of $1 \times 1\,\mathrm{mm}^2$. The ^{11}Be beam energy was measured event by event from the Time of Flight (ToF) between a plastic scintillator and the PPACs along a flight path of ~ 5 m. The ToF was energy calibrated via a 500 μm Si detector which could be inserted immediately after the PPACs. The accuracy of this procedure was estimated around 4%. The ^{11}Be beam energy distribution turned out to be bell shaped and peaked around 43 MeV with a FWHM of ~ 18 MeV and a total intensity of $\sim 10^5$ pps.

The ^{11}Be scattering events were detected with the EXODET array [6]. This setup consists of $4+4$ ΔE (40 μm)-E_{res} (500 μm) Si telescopes, each one with a surface of $5 \times 5\,\mathrm{cm}^2$, arranged along the faces of two cubes closely packed around the target. The E_{res} (ΔE) detector energy resolution was $\sim 1\%$ (5%). Each detector was segmented in 100 strips 0.5 mm wide. The strips of the ΔE layer were perpendicular to those of the E_{res}, allowing a pixel resolution of $0.5 \times 0.5\,\mathrm{mm}^2$. The whole array covered, for a point-like source, the polar angle ranges 26°–82° and 98°–154° with a total solid angle coverage of $\sim 2\pi$ sr. The ^{209}Bi target was $3.0\,\mathrm{mg/cm}^2$ thick with a 1 μm mylar backing and had a diameter of ~ 5 cm. This large surface was needed since the ^{11}Be beam distribution on the target had a Lorentzian shape with a FWHM of ~ 3 cm $(x) \times 2$ cm (y). An event-by-event tracking of the incoming particles together with the knowledge of the EXODET hit pixel was necessary to reconstruct the scattering angle. The angular divergence of the beam at the target site was $\sim 1°$ and therefore neglected in the subsequent analysis. The uncertainty in the θ-angle reconstruction originating from the position resolution of the two PPACs and the telescopes was estimated to be $\sim 2°$ and negligible when compared to the θ binning of 10° adopted in the analysis for statistical accuracy reasons.

The data acquisition system was triggered by the "OR" of the energy signals coming from the 8 ΔE Si detectors. The recorded events were: a) the time signals necessary for the ToF measurement of the incoming particles, b) the PPACs signals for the (x, y) beam position identification, c) the energy signals from each EXODET detector, d) the digital information processed by the ASIC chip: i) hit strip number, ii) Jitter Time (JT), iii) Time over Threshold (ToT) [6]. These last two quantities were useful to suppress spurious and trigger uncorrelated events and to get a coarse discrimination of the high-energy events (^{11}Be scattering) from the low-energy ones (protons, β-rays, γ-rays).

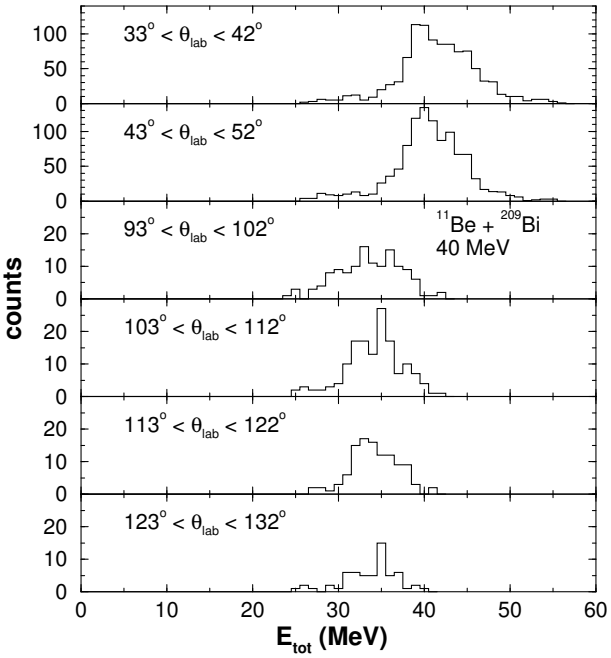

Fig. 1. Samples of high-energy events spectra at 40 MeV ^{11}Be beam energy. The large energy spread is due, in addition to the beam energy binning and target thickness, also to the energy resolution of the ΔE and E_{res} detectors signals added to reconstruct the total energy.

In this work we selected a 2 MeV beam energy bin centered around 40 MeV, close to the maximum of the energy distribution (corresponding to a beam intensity $\sim 2 \times 10^4$ pps) and another around 38 MeV (with a factor-2 lower intensity) for normalization purposes. This binning corresponds to a total energy resolution, including the target thickness, of 5%. Due to this limitation in the energy resolution the experimental data include the possible excitation of the first ^{11}Be excited state at 0.32 MeV and of the ^{209}Bi states up to ~ 2.6 MeV. Figure 1 shows some examples of the collected events.

The counting rate $N(\overline{\theta})$ measured at an average polar angle $\overline{\theta}$ is related to the average differential cross-section $\frac{\mathrm{d}\sigma}{\mathrm{d}\Omega}(\overline{\theta})$, solid angle $\Delta\Omega(\overline{\theta})$, average detector efficiency $\overline{\eta}(\overline{\theta})$, target areal density T and beam intensity B, by the classical formula: $N(\overline{\theta}) = \frac{\mathrm{d}\sigma}{\mathrm{d}\Omega}(\overline{\theta}) \cdot \Delta\Omega(\overline{\theta}) \cdot \overline{\eta}(\overline{\theta}) \cdot T \cdot B$. If $\Delta\Omega(\overline{\theta})$ is known (from Monte Carlo simulation in our case), one can usually get the unknown cross-section $\frac{\mathrm{d}\sigma}{\mathrm{d}\Omega}(\overline{\theta})$ comparing the data with those from a known cross-section, typically the Rutherford scattering at forward angles, under the assumption that the detector efficiency is the same at the same angle. The EXODET array gives positions from 80000 pixels [8(telescopes) $\times$ 100(ΔE strips) $\times$ 100(E_{res} strips)], allowing to reconstruct the θ scattering angle. In our setup the pixel efficiency resulted to be sometimes significantly different from pixel to pixel;

Table 1. Differential cross-sections for quasi-elastic scattering in the system $^{11}\mathrm{Be} + {}^{209}\mathrm{Bi}$ at 40 MeV.

$\overline{\theta}_{cm}$	Angular range (lab.)	$\frac{\mathrm{d}\sigma}{\mathrm{d}\sigma_{Ru}}$	$\Delta\left(\frac{\mathrm{d}\sigma}{\mathrm{d}\sigma_{Ru}}\right)$
30°	23°–32°	0.82	0.12
40°	33°–42°	1.00	0.11
50°	43°–52°	1.00	0.11
61°	53°–62°	0.87	0.10
71°	63°–72°	0.76	0.09
101°	93°–102°	0.82	0.14
111°	103°–112°	0.71	0.12
121°	113°–122°	0.80	0.14
130°	123°–132°	0.68	0.16
140°	133°–142°	0.59	0.19

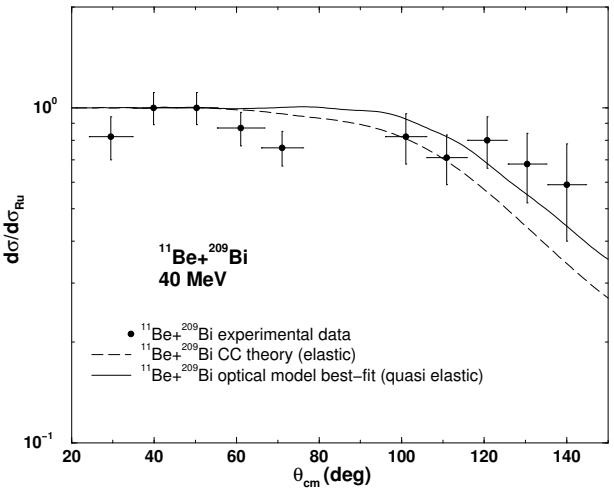

Fig. 2. Experimental angular distribution and relative optical model fits (see text for more details).

this was originating mainly from the noise out of the ASIC chip. This problem was faced into two different ways. In the first approach the 40 MeV data were normalized to those at 38 MeV, where from a semi-classical point of view the cross-section is expected to be purely Rutherford at all angles, since the Coulomb barrier is nominally higher ($V_{C_{Lab}} = 39.5$ MeV). Actually, from a quantum-mechanical description, some small absorption at very backward angles cannot be excluded. This was evaluated with the code FRESCO [14] within the optical model framework. We used a Woods-Saxon potential with the standard Akyüz-Winther parameterization [15]: $V_0 = W_0 = 52.328$ MeV, $r_0 = r_w = 1.194$ fm, $a_0 = a_w = 0.63$ fm. We verified that there was no significant variation in the evaluated cross-sections after a variation of ±50% in the potential depth and of ±0.05 fm in radius and diffuseness. The final values for $\mathrm{d}\sigma/\mathrm{d}\sigma_{Ru}$ at 38 MeV were: 1.00 up to 90°, 0.97 (at 100°), 0.93 (at 110°), 0.88 (at 130°) and 0.82 at (140°). These values were adopted to renormalize the angular distribution at 38 MeV. In the second approach the data were normalized to the three most forward angles where the scattering is purely Rutherford. The effective solid angles covered by the setup were evaluated both by Monte Carlo simulations and using analytical formulas, while strip efficiency was evaluated with standard alpha sources. The results of the previous approach were confirmed within the statistical accuracy. The $\mathrm{d}\sigma/\mathrm{d}\sigma_{Ru}$ values at 40 MeV are listed in table 1 and plotted in fig. 2. The quoted errors originate for the x-axis from the angular binning $\Delta\theta = 10°$ which had to be adopted, and for the y-axis from the statistical accuracy of the data and the beam energy bin of 2 MeV.

The data analysis was focused on the evaluation of the σ_{re}. Since the data, due to the experimental resolution, are relative to the quasi-elastic scattering, the analysis was performed in two steps. At first the data were fitted according to a Woods-Saxon parametrization of the interaction potential. The initial values of the six fitting parameters were as previously the standard Akyüz-Winther ones [15]. The best fit was achieved with the following set: $V_0 = 52.328$ MeV, $W_0 = 92.715$ MeV, $r_0 = r_w = 1.194$ fm, $a_0 = a_w = 0.63$ fm, and $\chi^2/N = 1.4$. The result is shown by a continuous line in fig. 2. An attempt to introduce in the fitting procedure the ^{11}Be halo feature did not produce realistic parameters. In the next step, using these best-fit potential values, we calculated, within the coupled-channel formalism, the differential cross-section for the pure elastic scattering (dashed line in fig. 2) with $\sigma_{re} = 555$ mb and for the excitation to the first ^{11}Be level ($1/2^-$ at 320 keV, $B(E1) = 0.115\,\mathrm{e^2fm^2}$ [16]) with $\sigma_1 = 251$ mb. The contributions arising from the unresolved ^{209}Bi excited states $7/2^-$ at 896 keV, $13/2^-$ at 1609 keV, and from the multiplet $[3^- \otimes h_{9/2^-}]$ at ~ 2.6 MeV were found to be very small, $\ll 1\%$, compared to the quasi-elastic cross-section. Higher excitations had even smaller cross-sections. This approach reproduced the experimental data. In order to have an evaluation of the σ_{re} uncertainties, the procedure was repeated assuming for $\overline{\theta}_{cm}$ the smallest values of table 1 angular ranges (smallest angle have potentially larger weight in the Rutherford differential cross-section). We got for σ_{re} an upper limit of 621 mb, consistent with the previous value, and σ_1 unchanged. From the performed fits we concluded that according to the limited statistics the experimental data do not show any significant effect coming from the ^{11}Be halo structure and there is only $\sim 50\%$ contribution to σ_{re} from ^{11}Be bound states, the rest originated, most likely, from the breakup process.

In order to get a deeper understanding of the present results, three systems with ^{9,10,11}Be, ^{17,19}F, and ^{4,6}He beams were compared near the Coulomb barrier. The scattering angular distributions are presented in fig. 3 and the relative σ_{re} data are listed in table 2. The σ_{re} for ^{11}Be (555 mb) was found to be larger than that for ^{9}Be (281 mb), but after the subtraction of the calculated contribution for the excitation to "unresolved" first and only bound ^{11}Be excited state ($\sigma_1 = 251$ mb), the two cross-sections are rather similar. This can be clearly seen in fig. 3 (top) where the solid line (elastic scattering + excitation of the ^{11}Be first excited state) is nearly overlapping with the short-dashed one (^{9}Be elastic scattering). Let us now make the assumption that in this energy range

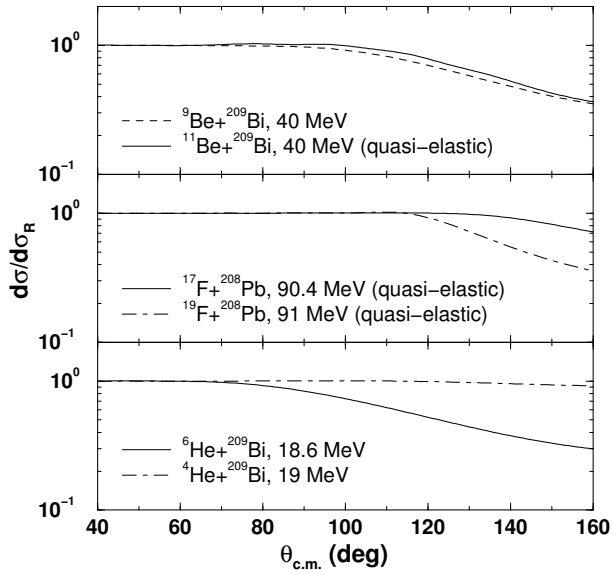

Fig. 3. Comparison of the differential angular distribution. The ^{19}F(^{4}He) data are from refs. [17,18]. See text for additional details.

Table 2. Reaction cross-section at Coulomb barrier energies; the barriers have been evaluated with $r_0 = 1.56$ [19,20].

System	E (MeV)	E_{cm}/V_C	σ_{re} (mb)	Ref.
^{9}Be + ^{209}Bi	40.0	1.00	281	[10]
^{10}Be + ^{208}Pb	39.0	0.99	5–26	[21]
^{11}Be + ^{209}Bi	40.0	1.01	555*	this work
^{17}F + ^{208}Pb	90.4	1.04	77	[6]
^{19}F + ^{208}Pb	91.0	1.05	269	[6]
^{4}He + ^{209}Bi	19.0	0.91	13	[4,5]
^{6}He + ^{209}Bi	18.6	0.91	662	[4,5]

* The calculated cross-section for the excitation of the ^{11}Be first (and only bound) excited state is 251 mb.

the absorption originates, in addition to the fusion process, mainly from the breakup. The consequence is, since the fusion cross-sections for both ^{9,11}Be are similar [11], that the breakup process in both nuclei have comparable strengths, and finally that the differences in binding energies and in nuclear-matter radii for ^{9,11}Be do not play a crucial role.

In the case of the F isotopes, the loosely bound ^{17}F presents much less absorption (fig. 3 middle) than the well bound ^{19}F, while the opposite situation happens for the two He isotopes, with a larger absorption for the weakly bound ^{6}He than for the stable ^{4}He (fig. 3, bottom). One possible explanation of these different behaviors, following what already discussed in ref. [6], is that collective excitations might play the most dominant role in the reaction dynamics around the Coulomb barrier for both well-bound and loosely bound projectiles. This explains why ^{19}F, with possible collective structure, has more absorption than ^{17}F, which has a well-known single-particle structure. On the other side, the absorption is smaller for ^{4}He than for ^{6}He, in fact ^{6}He has an unbound 2^+ state at ~ 1.8 MeV (with a possible collective nature), whereas ^{4}He first excited state is at 28 MeV. Finally, the fact that for both Be isotopes the contributions to the σ_{re} due to excitations to "not-bound" states are rather similar could be attributed to the "similar" collective nature of the two nuclei. In fact both Be isotopes have a strongly deformed ^{8}Be core, which produces in case of ^{9}Be a g.s. rotational band with an experimental $\beta_2 = 1.00$ [11]. Moreover, also from a theoretical point of view [22], similar deformations have been foreseen for ^{9}Be and ^{11}Be. The σ_{re} of ^{10}Be (see table 2) is in agreement with this interpretation since in this nucleus, with $S_n = 6.8$ MeV, the breakup process should be much smaller and moreover the fusion cross-section (measured with a ^{209}Bi target [11]) is also in this case similar to the ^{9,11}Be ones (also the quoted values at $E_{cm}/V_C = 1.2$, $\sigma_{re} = 207$–220 mb [21], do not contradict this conclusion). We underline that this is only one possible explanation of the results since: i) the absorption could originate, in addition to the fusion process, not only from the breakup but also from other alternative direct processes as 2-neutron transfer (reported for ^{6}He [23]), ii) the different penetrabilities of the breakup - protons (neutrons) in the F (He, Be) case through the nucleus barrier could influence the breakup process in a different way. These first generation experiments point to the need of more accurate experiments, once beams with better qualities will be available.

In summary, for the first time the scattering differential cross-section was measured for the system ^{11}Be + ^{209}Bi at one energy around the Coulomb barrier, overcoming the considerable problems related to low intensity and poor emittance of the ^{11}Be secondary beam. The success of the measurement was also due to the high efficiency and granularity of the EXODET. Both, the low binding energy and the halo structure in ^{11}Be do not seem to play a big influence on the reaction dynamics at the Coulomb barrier, since σ_{re} of ^{11}Be results to be very similar to that of ^{9}Be. A comparison of similar systems ^{11,9}Be + ^{209}Bi, ^{17,19}F + ^{208}Pb and ^{4,6}He + ^{209}Bi might suggest that in this energy domain the inelastic excitations dominated by nuclear-structure effects play an overwhelming role. ^{10}Be + ^{208}Pb data support this interpretation too.

The authors thank C. Beck for a critical reading of a first version of this paper.

References

1. K. Hagino *et al.*, Phys. Rev. C **61**, 037602(R) (2000).
2. A. Diaz-Torres *et al.*, Phys. Rev. C **65**, 024606 (2002).
3. I. Tanihata *et al.*, Phys. Rev. Lett. **55**, 2676 (1985).
4. E.F. Aguilera *et al.*, Phys. Rev. C **63**, 061603(R) (2001).
5. E.F. Aguilera *et al.*, Phys. Rev. Lett. **84**, 5058 (2000).
6. M. Romoli *et al.*, Phys. Rev. C **69**, 064614 (2004).
7. K.E. Rehm *et al.*, Phys. Rev. Lett. **81**, 3341 (1998).
8. J.F. Liang *et al.*, Phys. Rev. C **67**, 044603 (2003).

9. C. Signorini *et al.*, Prog. Theor. Phys. Suppl. **154**, 272 (2004).
10. C. Signorini *et al.*, Phys. Rev. C **61**, 061603(R) (2000).
11. C. Signorini *et al.*, Nucl. Phys. A **735**, 329 (2004).
12. T. Kubo *et al.*, Nucl. Instrum. Methods Phys. Res. B **70**, 490 (1992).
13. H. Kumagai *et al.*, Nucl. Instrum. Methods Phys. Res. A **470**, 562 (2001).
14. I.J. Thompson, Comput. Phys. Rep. **2**, 167 (1998).
15. R. Broglia, A. Winther, *Heavy Ion Reactions* (Addison-Wesley, 1990) p. 113.
16. F. Ajzenberg-Selove, Nucl. Phys. A **506**, 1 (1988); T. Nakamura *et al.*, Phys. Lett. B **394**, 11 (1997).
17. C.J. Lin *et al.*, Phys. Rev. C **63**, 064606 (2001).
18. A.R. Barnett *et al.*, Phys. Rev. C **9**, 2010 (1974).
19. M. Dasgupta *et al.*, Phys. Rev. Lett. **82**, 1395 (1999).
20. C. Signorini *et al.*, Eur. Phys. J. A **5**, 7 (1999).
21. J.J. Kolata *et al.*, Phys. Rev. C **69**, 047601 (2004).
22. A. Doté *et al.*, Phys. Rev. C **56**, 1844 (1997).
23. P.A. De Young *et al.*, Phys. Rev. C **71**, 051601 (2005).